Estimation of anisotropy parameters from surface passive seismic data

Davide Gei*, Leo Eisner† and Peter Suhadolc‡

*Istituto Nazionale di Oceanografia e di Geofisica Sperimentale (OGS), Trieste, Italy
†Institute of Rock Structure and Mechanics, Academy of Sciences of the Czech Republic
‡Department of Geosciences, University of Trieste, Italy

Introduction

Microseismic data recorded by surface monitoring arrays can be used to estimate the effective anisotropic parameters of the overburden and reservoir. In this study we use P- and SH-wave arrival-time inversions to estimate the Thomsen parameters ε, δ and γ. The inversions consider two analytic equations of P- and SH-wave arrival times as a function of offset in a homogeneous media with a vertical axis of symmetry (VTI) (e.g. Grechka and Tsvankin, 1998; Grechka, 2009). VTI media are characterized by non-hyperbolic reflection moveout, more significant in large-offset arrivals for q-P and q-S waves.
In this study we compute the effective Thomsen parameters from passive seismic data acquired during the hydraulic fracturing of a gas-shale reservoir located in Oklahoma (USA).

P- and SH wave traveltime inversion for homogeneous transverselly isotropic media

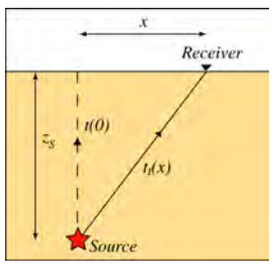

Figure 1 Schematic representation of a passive seismic monitoring experiment. The source is located at a depth z_S and the receiver at an offset x. $t_t(x)$ is the traveltime and $t(0)$ is the one-way vertical traveltime.

The nonhyperbolic moveout of P-waves for a single horizontal transversely isotropic medium with a vertical symmetry axis (VTI) can be expressed by (Alkhalifah and Tsvankin,1995):

$$t_t^2(x) = t^2(0) + \frac{x^2}{V_{NMO}^2} - \frac{2\eta x^4}{V_{NMO}^2\left[t^2(0)V_{NMO}^2 + (1+2\eta)x^2\right]}, \quad (1)$$

where, for microseismic applications, $t(0)$ is the one-way vertical time, x is the offset (surface projection of the source-receiver dist $\eta = (\varepsilon - \delta)/(1+2\delta)$ is the anellipticity parameter and V_{NMO} is the normal-moveout velocity. ε and δ are two Thomsen (1986) anisotropy parameters. Figure 1 shows a shematic representation of the wave propagation in a homogeneous medium.The NMO

$$V_{NMO}^2 = V_{P0}^2(1+2\delta), \quad (2)$$

where V_{P0} is the vertical P-wave velocity. For passive seismic monitoring, the measured arrival time $t_a(x)$ is given by:

$$t_a(x) = t_t(x) + t_0, \quad (3)$$

where $t_t(x)$ is the traveltime in the subsurface and t_0 is the origin time. Theoretical P-wave arrival times can be computed with equations 1 for given values of t_0, δ and η. V_{P0} and the source depth z_S are considered known quantities. The inversion algorithm is based on minimizing the root mean square (RMS) of time residuals, the time series given by the difference between the measured and computed arrival times.

The SH-wave arrival time inversion is based on the same Eq (3) but the traveltime $t_t(x)$ is given by:

$$t_t(x) = \sqrt{x^2 + z_S^2}\,\frac{\sqrt{1+2\gamma\cos^2\phi}}{V_{S0}\sqrt{1+2\gamma}}, \quad (3)$$

where V_{S0} is the vertical S-wave velocity and $\phi = \arctan(x/z_s)$

Experiment design

In 2008 Microseismic Inc. acquired a seismic dataset during the hydraulic stimulation of the Woodford shale. The unconventional reservoir, located in Oklahoma (USA), is operated by Newfield Exploration Mid-Continent Inc. The main goal of this microseismic monitoring was to locate the events produced by the fracking. The survey pattern, specifically designed for this purpose, consists of a 10-line Fracstar® array with 1C geophones (vertical component) located on the Earth's surface (Figure 2). The number of receivers per arm varies between 54 (line four) and 122 (lines 2 and 10) and the average receiver distance is 23 m.

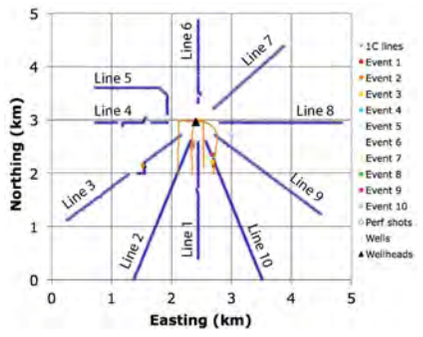

Figure 2 Plan view of the star-like array of 1C geophones (blue crosses). The black triangle in the center represents the wellheads and the orange curves show the wells trajectory. Diamonds and circles indicate the locations of microseismic events and perforation shots, respectively.

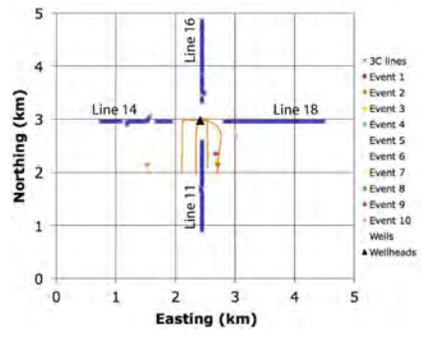

Figure 3 Plan view of the four 3C lines. The blue crosses represent the accelerometers. The black triangle in the center represents the wellheads and the orange curves show the wells trajectory. The circles indicate the locations of microseismic events.

Microseismic Inc. deployed 4 additional lines of three-components accelerometers (Figure 3) approximately coinciding with four of the 1C seismic lines. All the accelerometers are planted with the same orientation, consisting in the magnetic North for the first horizontal component and East for the second one.
The pay interval, located at the approximate depth of 2 km, is probed by 4 horizontally deviated wells, having the wellheads in the center of the star-like array of receivers.

Inversion of perforation shots

In this section we consider the inversion of the P-wave arrival times picked from four perforation shots whose locations are indicated by red diamonds in Figure 2. Figure 4 shows the 1D P-wave velocity profile of the study area and the effective velocity at the perfs depth. At 2100 m, depth of the perforation shots analyzed in this section, the effective P-wave velocity is V_{P0}=2906 m/s.
Figure 5 shows examples of picking the first arrivals (red curves). The seismic signals from lines 4-6 are too weak to be pickable for any perforation shot analyzed in this study. The linear signals parallel to the dashed lines represent tube waves which, after traveling up the wellbore, spread out over the Earth's suface generating P- (green) and Rayleigh-waves (yellow).
Panels a) and b) of Figure 6 show the picked arrival times of Shots 1 and 2 and panels c) and d) represent residual times, the difference between picked and the analitic arrival times, the latter computed with Equations (1) and (3).

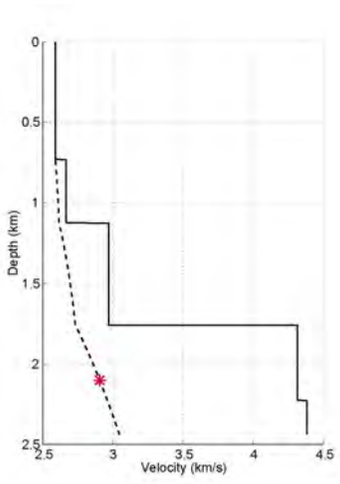

Figure 4 1D vertical P-wave velocity profile of the study area. The interval velocity is given by the continuous line and the dashed line is the effective vertical velocity. The red asterisk represents the effective velocity of the perforation shots.

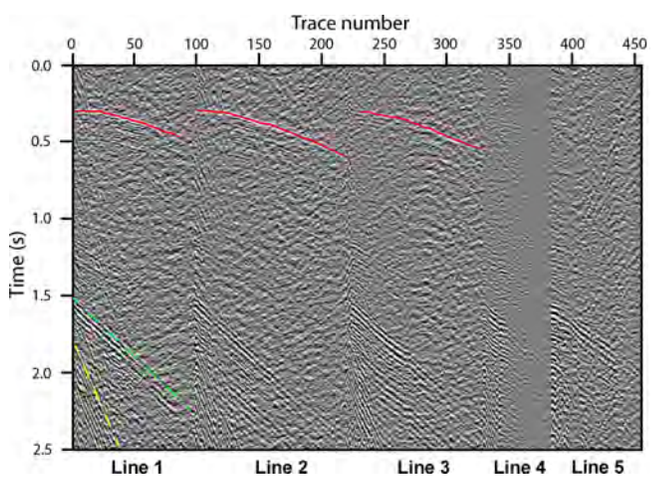

Figure 5 Seismic lines 1-5 of perforation shot 3, stage 3, well 5H. Picked first arrivals are indicated by red curves. See Figure 2 for numbering and location of seismic lines.

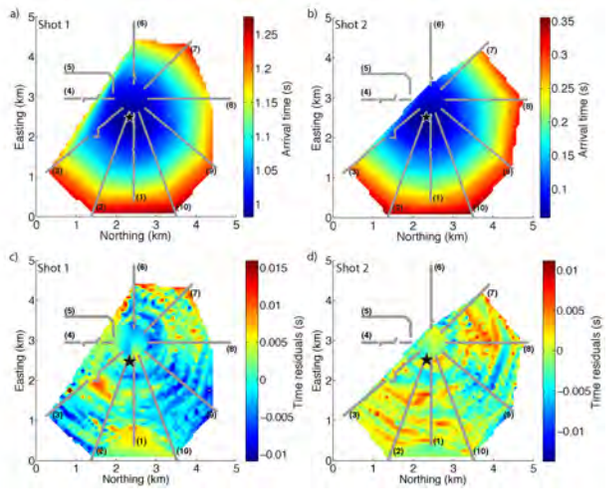

Figure 6 Contour plots of the picked arrival times from shots 1and 2 (panels a and b) and residuals times for the same shots (panels c and d). The straight, gray, numbered lines represent the 10 arms of the Fracstar. The black stars represent the source locations.

Inversions of arrival times in isotropic layered media can result in apparent anisotropy. To estimate the influence of layering on the above inverted effective anisotropy we compute and invert synthetic arrival times for a layered isotropic medium. We consider a horizontally layered model suitable for this data set with the P-wave velocity profile shown in Figure 4 (continuous line) and, compute the synthetic traveltimes in the isotropic layered model and add Gaussian noise with zero mean and standard deviation of 4 ms, similar to the residuals observed in the inversions of the field data. Table 1 shows the inverted anisotropic parameters. For the synthetic dataset they are only about 50% of the parameters observed in the inversion of the real data set, assuming a homogeneous medium. Consequently, the isotropic layers seem to cause only about 50% of the effective anisotropy, indicating that the reservoir or one of the layer forming the overburden are intrinsically anisotropic.

Table 1 Results of P-wave arrival time inversions of field data (after Gei et al., 2011); the term isotropic refers to the synthetic dataset of the layered medium.

	t_0 (s)	δ	η	ε	RMS (ms)
Shot 1	-0.256	0.117	0.273	0.454	4.0
Shot 2	0.666	0.121	0.264	0.449	3.4
Shot 3	0.433	0.121	0.276	0.464	3.3
Shot 4	-0.118	0.136	0.222	0.418	4.4
Isotropic	0.001	0.012	0.115	0.130	4.3

P-wave arrival time inversion of microseismic events

Among the few hundreds microseismic events recorded during the hydraulic fracturing of the gas shales, we consider 10 events producing the stronger seismic signal. We estimate the Thomsen anisotropy parameters δ and ε from the P-wave first arrivals picked on the 1C geophones seismograms. The P-wave arrival times inversion is based on Equations (1) and (3). An example of picking of first arrivals is shown in Figure 7, where the Event 7 is considered.

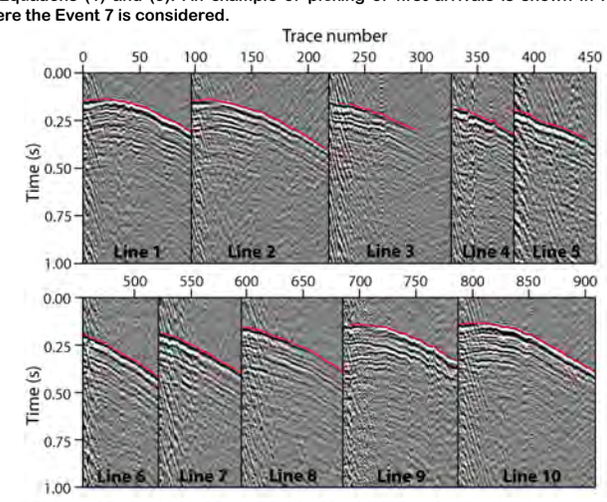

Figure 7 Picking of first arrivals of Event 7 for the 10 seismic lines forming the star array.

Comparisons between experimental and synthetic arrival times for homogeneous isotropic and anisotropic media are shown in Figure 8. In panels a) and c), the mismatching between the synthetic and experimental arrival times given by red and blue dots, respectively, clearly indicates that the medium is not isotropic. Instead panels b) and d) show a good matching between experimental and synthetic arrival times for a VTI medium with properties given in Table 2.

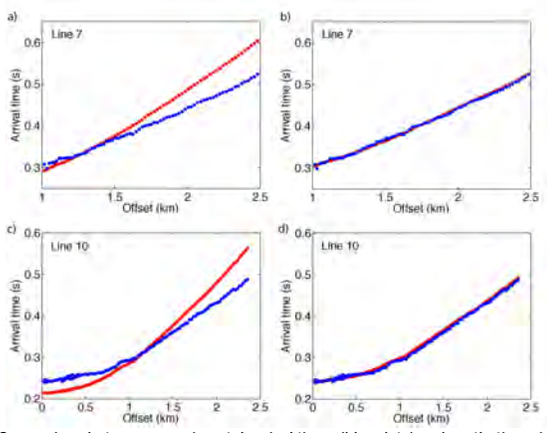

Figure 8 Comparison between experimental arrival times (blue dots) and synthetic arrival times (red dots) for lines 7 and 10 of Event 7. In panels a) and c) the synthetic data correspond to an isotropic medium, while in panels b) and d) the symmetry of the medium is VTI with the parameters given in Table 2.

Figure 9 describes the P-wave arrival time inversion of Event 7. Panels a) and b) show contour plots of the the picked arrival times (1C dataset) and of the the residual times, respectively. The white stars represent the source location. Panel c) shows the time residuals as a function of offset and each color of the circles represents a different arm of the star-like array. The analysis of the time residuals of the whole dataset (10 events) do not indicate azimuthal dependence of the time residuals, confirming a VTI symmetry.

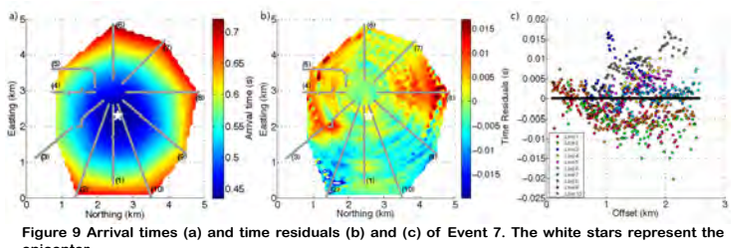

Figure 9 Arrival times (a) and time residuals (b) and (c) of Event 7. The white stars represent the epicenter.

The results of the P-arrival time inversion of Events 1-10 are given in Table 4.8. δ, ε and η are the results of the inversion and have average values of 0.14, 0.41 and 0.22, respectively. These figures are consistent with the inversions of perforation shots (Table

Table 2 Results of P-wave arrival time inversions of microseismic events with data acquired with the 10 star-like array configuration.

	t_0 (s)	δ	η	ε	RMS (ms)
Event 1	-0.184	0.125	0.226	0.408	5.3
Event 2	0.155	0.116	0.224	0.392	14.4
Event 3	-0.491	0.112	0.199	0.356	5.4
Event 4	0.270	0.200	0.156	0.418	5.1
Event 5	-0.519	0.166	0.179	0.404	7.0
Event 6	-0.093	0.016	0.450	0.480	10.3
Event 7	-0.283	0.165	0.190	0.418	5.6
Event 8	0.018	0.191	0.154	0.404	6.7
Event 9	-0.232	0.178	0.176	0.417	4.9
Event 10	0.214	0.087	0.254	0.385	4.5

SH-wave arrival time inversion of microseismic events

In a VTI medium the SV- and SH-waves can be separated considering the radial and transverse components, respectively, resulting from the backazimuth rotation of the horizontal components of each receiver. The SH-waves first arrival times can be picked on the transverse component and inverted with Equation 3 to estimate the Thomsen parameter γ. An example of picked SH-waves arrival times is given in Figure 10.

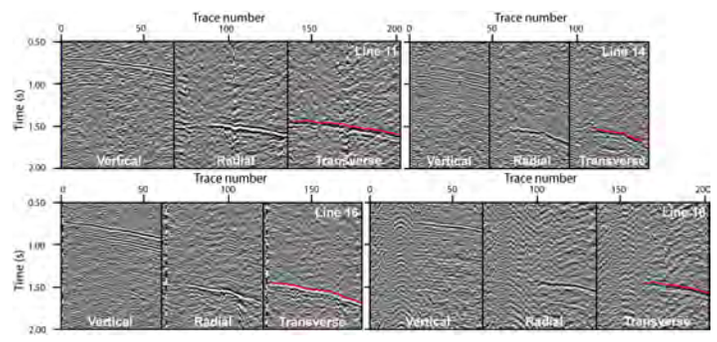

Figure 10 Vertical, Radial and Transverse components of lines 11, 14, 16 and 18 of Event 6. The red curves represent picking times of SH-waves.

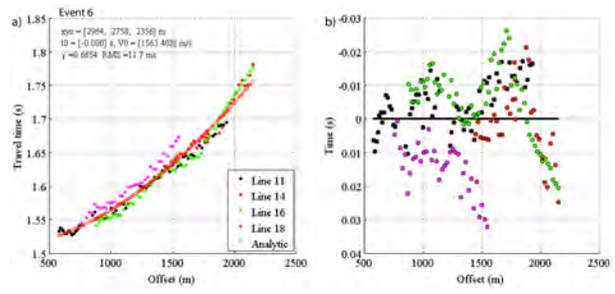

Figure 11 a) Analytic SH-waves arrival times (red empty circles) best fitting the picked arrival times for Event 6 (filled circles); b) time residuals for lines 11 (black), 14 (red), 16 (green) and 18 (magenta).

Figure 11 shows the inversion of Event 6, where panel a) shows the comparison of the picked- (filled circles) with the synthetic- arrival-times (empty red circles) computed with the best estimate of V_{S0} and γ, while the right panels are time residuals of lines 11, 14, 16 and 18 vs offset. Table 3 shows the results of the SH-wave arrival time inversions of Events 1-10 where the estimated Thomsen parameter γ show high but consistent values.

Table 3 Results of SH-wave arrival time inversions of microseismic events.

Event #	1	2	3	4	5	6	7	8	9	10
γ	0.64	0.60	0.64	0.64	0.64	0.67	0.78	0.63	0.74	0.57
v_{S0} (m/s)	1479	1480	1499	1463	1460	1563	1460	1454	1458	1534
RMS (ms)	11.1	17.5	7.5	10.8	16.7	11.7	11.3	8.8	6.1	23

Conclusions

This study, focuses on the arrival times inversions of P- and SH-waves from microsesimic data acquired during the hydraulic fracturing of a gas shale formation located in Oklahoma (USA). The analysis of P-wave arrival times reveals that VTI symmetry characterizes the study area. The inversion algorithm is based on the minimization of the difference between experimental and theoretical traveltimes, the latter defined for homogeneous VTI media.
The inversions of P-wave arrival times from perforation shots give consistent results and suggest a relatively strong anisotropy characterizing the reservoir and/or the overburden. These results are confirmed by the inversion of compressional waves arrivals related to microseismic activity, although the anisotropy parameters show higher dispersion if compared with the parameters obtained from the perforation shots.
The SH arrival times are much worse fitted than P-wave arrival times and show significant residuals depending on offset. However they suggest highly consistent and intense anisotropy.
The parameters obtained in this study are relatively high but are expression of effective and not intrinsic anisotropy.

References

Alkhalifah, T., and Tsvankin, I., 1995, Velocity analysis for transversely isotropic media, Geophysics, 60, 1550-1566.

Gei, D., and Eisner, L., and Suhadolc, P., 2011, Feasibility of estimating vertical transverse isotropy from microseismic data recorded by surface monitoring arrays, Geophysics, 76, 117-126.

Grechka, V., 2009, Applications of Seismic Anisotropy in the Oil and Gas Industry, EAGE Publications, 171 pp., ISBN 978-90-73781-68-9.

Grechka, V., and Tsvankin, I., 1998, Feasibility of nonhyperbolic moveout inversion in transversely isotropic media, Geophysics, 63, 957-969.

Thomsen, L, 1986, Weak elastic anisotropy, Geophysics, 51 (10), 1954-1966.

Acknowledgments

I am very grateful to the Newfield Exploration Mid-Continent Inc. for advice and for providing data. I also thank Microseismic Inc. for the data and support provided for the data management (including the picking software). Special thanks to Vladimir Grechka for guidance, suggestions and discussions.